Korean J. Chem. Eng., 36(12), 2023-2034 (2019)
DOI: 10.1007/s11814-019-0382-z

pISSN: 0256-1115
eISSN: 1975-7220

A combined experimental and theoretical investigation of the adsorption of 4-Nitrophenol on activated biocarbon using DFT method

Aola Supong, Parimal Chandra Bhomick, Upasana Bora Sinha, and Dipak Sinha†

Department of Chemistry, Nagaland University, Lumami-798627, India
(*Received 16 May 2019 • accepted 2 September 2019*)

Abstract−Porous activated biocarbon from Ravenna grass was utilized as an adsorbent for the removal of 4-Nitrophenol from aqueous solution. Chemical activation process using potassium hydroxide was adopted for the activated biocarbon preparation. The essential features of the prepared adsorbent represented by BET surface area, pore volume and pH_{ZPC} were 919 m^2g^{-1}, 0.324 cm^3g^{-1} and 8.1 respectively. SEM, FTIR, XRD and TGA analysis revealed the microcrystallite and porous structure of the synthesized biocarbon with abundant functional groups and high thermal stability. Batch adsorption tests were conducted for 4-Nitrophenol adsorption, and the optimum adsorbent dose, pH, initial 4-Nitrophenol concentration and contact time were found to be 0.5 g, 7, 400 mgL^{-1} and 40 minutes, respectively. The equilibrium isotherm study revealed the suitability of the Langmuir isotherm with a maximum adsorption capacity of 50.89 mg/g. The pseudo-second-order kinetic model well represented the adsorption kinetics data, while thermodynamics study indicated the spontaneity ($\Delta G<0$) and endothermic nature ($\Delta H>0$) of the adsorption of 4-Nitrophenol. Density functional theory (DFT) calculations performed at the B3LYP level indicated that the interaction of 4-Nitrophenol with pristine and functionalized activated biocarbon is favorable.

Keywords: Activated Biocarbon, Ravenna Grass, Chemical Activation, 4-Nitrophenol, DFT

INTRODUCTION

The generation and discharge of wastewaters have increased drastically in recent years, limiting the availability of save and clean drinking water. Large quantities of wastewater containing toxic pollutants are generated from different types of industries, and the greatest environmental challenge is the removal of these harmful pollutants from wastewaters. Phenolic compounds constitute a major group of hazardous pollutant, and among them, 4-Nitrophenol is considered as one of the priority pollutants since its presence in even minute concentrations can bring serious harm to human beings, animals and aquatic systems [1]. The main cause of pollution by 4-nitrophenol in waterbodies is the untreated effluent discharged from different types of industries such as oil refineries, pharmaceuticals, textiles, steel mills, petrochemicals, plywood industries, insecticides production unit, coke processing units, resin plants, pulp and paper industries, among others [2]. Human contact with 4-Nitrophenol can leave acute as well as chronic impacts, such as vomiting, sore throat, kidney damage, liver and gastrointestinal tract, difficulty in swallowing, skin and eye irritation, cardiovascular diseases, protein degeneration, central nervous system disorder, salivation, anorexia, fainting, tissue erosion, muscle weakening, and vertigo [3-6]. Therefore, it is very much necessary to treat wastewater loaded with 4-Nitrophenol before releasing into water bodies. Over the years, extensive research has been going on to address the issue, and several conventional and advanced technologies have been adopted for the safe treatment of wastewater containing 4-Nitrophenol. These include adsorption and extraction [7,8] distillation [9,10], membrane processes [11,12], electrochemical oxidation [13,14], chemical oxidation [15,16], advanced oxidation process [17-20], biological treatment [21,22] and enzymatic treatment [23,24]. Among all the available methods, adsorption using activated biocarbon remains as one of the best choices because of its efficiency and ability to remove not only one but all types of phenolic compounds from wastewater. The multifaceted characteristics of activated biocarbon such as high surface area, good thermal stability, large pore volume, abundant surface functional groups, lack of production of secondary by-products, simple design and easy operation make them one of the most prolific adsorbents. This versatile adsorbent can be synthesized via physical activation, chemical activation and physicochemical activation [25]. Although activated biocarbon has its many advantages, the utilization of fossil-based precursors or coal in the production of commercial activated carbon increases the cost. Therefore, this has prompted many researchers to use alternative, cost-effective raw precursors to counteract the limitations of commercial activated carbon. Over the years, many low cost activated biocarbons have been produced and used for a wide variety of applications. For example, hazelnut shell derived activated carbon was utilized for the removal of tetracycline antibiotics [26], corn-cob based nitrogen-doped activated carbon was used for high energy hybrid supercapacitor [27], Sulfonated activated carbon from coffee residue was used for esterification as a green catalyst [28]. Mullick et al. synthesized low-cost rice husk-based activated carbon for the hexavalent chromium removal [29], You et al. used hazelnut shell derived activated carbon as binding agents in DGT samplers for sampling and measurement of nitrophenols in wastewater [30].

†To whom correspondence should be addressed.
E-mail: dipaksinha@gmail.com

Certain reports are also available indicating the utilization of cost-effective activated biocarbon for the adsorptive removal of phenolic compounds, such as 4-Nitrophenols [3,31-35], which provides an impetus for further study in this area. These adsorption experiments have been found to depend on factors such as the nature of the activated biocarbon and adsorption conditions. In recent years, various attempts have also been made to comprehend the adsorption process theoretically through density functional theory (DFT). Numerous studies relating to the theoretical understanding of adsorption interactions of various pollutant such as phenol [36], H_2S [37], mercury [38], CO_2 [39], bisphenol A [40], SO_2 [41] with activated carbon using DFT have been reported. The application of DFT in adsorption studies would provide a clear understanding of the adsorption phenomenon under study. However, almost no work has been reported on the theoretical studies of the interaction of 4-Nitrophenol with activated biocarbon. Therefore, an attempt has been made in this study to understand the possible interactions taking place between 4-Nitrophenol and the activated biocarbon surface during the adsorption process. Such studies would not only improve our understanding of the bonding and reactivity between the adsorbate and adsorbent but also help in designing an effective adsorbent for 4-Nitrophenol removal.

Thus, keeping all this in mind, the present study focussed on the preparation of cost-effective activated biocarbon from an invasive grass-Ravenna grass through chemical activation method. Several analytical techniques were used to examine the morphological characteristics of the activated biocarbon. Batch adsorption studies of 4-Nitrophenol were carried out to test the efficacy of the prepared carbon and the experimental data were fitted to adsorption isotherm and kinetics models. Theoretical calculations using DFT were employed to understand the interaction of 4-Nitrophenol with pristine and functionalized activated biocarbon.

The novelty of the present work lies in the conversion of an invasive and noxious grass-Ravenna grass into a low-cost activated biocarbon and its effective application in the removal of toxic 4-nitrophenol from aqueous solution. In addition, theoretical calculations using DFT provided an understanding of the possible interaction of 4-Nitrophenol with the activated biocarbon. DFT studies also provided an insight into the effect of different functional groups such as OH, CHO and COOH on the adsorption process. Such studies help in selecting the appropriate chemical activating agent to modify the carbon surface so as to obtain the maximum adsorptive removal of 4-Nitrophenol.

MATERIALS AND METHOD

1. Ravenna Grass Activated Biocarbon Preparation

The raw material Ravenna grass was collected locally (26°16′23″N| 94°27′55″E). The whole plant was used for the production of activated biocarbon. The biomass was washed and placed in an oven at 110 °C for 12 hours. The dried biomass was carbonized at 400 °C for 1 hour, and the obtained char was further ground into a uniform fine powder. The powdered char was further subjected to chemical activation using KOH as the activating agent. For chemical activation, 20 g of the powdered char was added to 250 ml of 1M potassium hydroxide solution (KOH), and the contents were magnetically stirred at 600 rpm for 3 hours at room temperature. The contents were then allowed to dry in an oven at 110 °C, and subsequently, the KOH impregnated char was activated at 700 °C for 1 hour using a muffle furnace at 10 °C min^{-1} heat flow rate. The sample was then rinsed with 0.1 M HCl and deionized water to attain a neutral pH and dried at 105 °C to obtain the Ravenna grass activated biocarbon (RABC).

2. Characterization of Ravenna Grass Activated Biocarbon

The physicochemical features of Ravenna grass activated biocarbon (RABC) were characterized by different analytical techniques. The surface area and pore volume of RABC were examined by Brunauer, Emmet and Teller (BET) analyzer (Smart instrument, SS93/02). Field-emission scanning electron microscopy (FESEM) was used to analyze the surface characteristics of RABC (FESEM, Model: ZEISS SIGMA MAKE: Carl ZEISS Microscopy, Germany). Thermogravimetric analysis (TGA-Perkin Elmer/STA-3000) was used to understand the thermal stability of RABC, while Fourier transform infrared spectroscopy (Spectrum Two, Perkin Elmer) helps in determining the various functional groups of RABC. XRD analysis was done using CuKα radiation at the scan rate of 0.2 degrees/minute (Rigaky-Ultimaiv Japan). The zero-point charge was determined by batch equilibrium test for activated carbon [42].

3. Batch Adsorption Study of 4-Nitrophenol

The efficiency of RABC to remove 4-Nitrophenol from aqueous solution was studied by batch mode equilibrium method. The effects of contact time, pH, initial concentration of 4-Nitrophenol, and adsorbent dose on the removal efficiency of 4-Nitrophenol by RABC were studied. For the batch study, 50 ml of 4-Nitrophenol solutions of different concentrations (100-500 mgL^{-1}) and pH ranging from 2 to 12 were contacted with different quantities of adsorbent dose (0.1-1 g). The mixtures were taken in a 250 ml Erlenmeyer Flasks and agitated at 180 rpm at a temperature of 25±2 °C for different contact time (0-180 minutes). The samples were then filtered, and the residual filtrate concentration of 4-Nitrophenol was analyzed using UV-VIS spectrophotometer (Perkin- Elmer lambda-35) at 317 nm wavelength. All the experiments were done in triplicate, and the average value of the three readings was reported. The adsorption capacity of 4-Nitrophenol and removal efficiency was determined by Eqs. (1) and (2), respectively.

$$q_e = \frac{(C_o - C_e)}{m} \times V \tag{1}$$

$$\text{Removal } \% = \frac{(C_o - C_e)}{C_o} \times 100 \tag{2}$$

where, q_e (mg/g) is the amount of 4-Nitrophenol adsorbed per unit mass at equilibrium, C_o (mg/L) is the initial concentration of 4-Nitrophenol, C_e (mg/L) is the equilibrium concentration, m (g) is the mass RABC and V (L) is the volume of the solution.

4. Adsorption Isotherm Models

The equilibrium adsorption behavior of 4-Nitrophenol onto the prepared RABC was investigated by Langmuir, Freundlich and Temkin adsorption isotherm models. The linear form of the models is given by Eqs. (3), (4) and (5), respectively.

$$\frac{C_e}{q_e} = \frac{1}{q_m} C_e + \frac{1}{q_m K_L} \tag{3}$$

$$\log q_e = \log K_F + \frac{1}{n}\log C_e \quad (4)$$

$$q_e = \frac{RT}{b_T}\ln C_e + \frac{RT}{b_T}\ln A_T \quad (5)$$

where, C_e=4-Nitrophenol concentration at equilibrium (mg L^{-1}), q_e=adsorption capacity of RABC at equilibrium (mg g^{-1}), q_m=maximum adsorption capacity (mg g^{-1}), K_L=Langmuir isotherm constant (L mg^{-1}), n=Freundlich adsorption intensity, K_F=Freundlich constant (mg g^{-1}) (L $mg^{-1})^{1/n}$, b_T=constant corresponding to heat of adsorption (kJ mol^{-1}), A_T=Temkin isotherm constant (L mg^{-1}), R=universal gas constant (8.314 J mol^{-1} K^{-1}) and T=Temperature (298 K).

5. Adsorption Kinetic Models

An experiment similar to equilibrium adsorption studies was done to study the kinetics of 4-Nitrophenol adsorption onto the RABC. For this study, 0.5 g of RABC was added to 50 ml of 4-Nitrophenol solution, and the mixture was agitated at a speed of 180 rpm for different time intervals at room temperature. Small amount of solution was taken at different time intervals and filtered, and the filtrate concentration at each interval was measured using a spectrophotometer. The kinetics of the adsorption of 4-Nitrophenol was studied by fitting the obtained experimental kinetics data to pseudo-first-order and pseudo-second-order model. The linearized form of the two models is given in Eqs. (6) and (7), respectively.

$$\log(q_e - q_t) = \log q_e - \frac{k_1}{2.303}t \quad (6)$$

$$\frac{t}{q_t} = \frac{1}{k_2 q_e^2} + \frac{1}{q_e}t \quad (7)$$

where, q_e=adsorption capacity at equilibrium (mg g^{-1}), q_t=adsorption capacity of RABC at time t (mg g^{-1}), k_1=pseudo-first-order-rate constant (min^{-1}), k_2=pseudo-second-order rate constant (g mg^{-1} min^{-1}).

6. Chi-squared Test

The selection of the best-fitted isotherm and kinetics model to the experimental data was validated by Chi-squared test (χ^2). The Chi-squared test is the sum of the squares of the differences between the experimental data and calculated data [43]:

$$\chi^2 = \Sigma_{i=1}^{n}\frac{(q_{e(exp)} - q_{e(cal)})^2}{q_{e(cal)}} \quad (8)$$

The χ^2 will be a small number, if the data calculated from various isotherm and kinetic models goes in line with the experimental data, whereas the χ^2 will be a large number if the calculated data varies from the experimental data.

7. Theoretical Study of 4-Nitrophenol Adsorption onto RABC

All the necessary theoretical calculations pertaining to the understanding of adsorption of 4-Nitrophenol onto RABC were carried out on Gaussian 09 [44] suite of programs. Density functional theory was implemented because of its simplicity and computational efficiency. The geometry optimization as well as frequency and energy calculations were performed at 6-31 g basis set and B3LYP hybrid functional in a dielectric medium of ε=80 (corresponding to water). To study the possible interaction of 4-Nitrophenol with RABC, it is necessary to create a reasonable structure for the activated biocarbon surface. Since activated biocarbon is considered as macrostructures with an aromatic cluster of different sizes, a benzene ring cluster model with armchair edge shapes was used to simulate the activated biocarbon surface in the present study [37]. The upper edge atoms of the cluster model were unsaturated to create an active site, whereas the carbon atoms on the remaining lower part of the cluster surface were terminated with hydrogen atoms. This unsaturated active site model was taken as pristine activated biocarbon. Besides, the active site was functionalized with OH, CHO and COOH groups to study the effect of such functional group on the 4-Nitrophenol adsorption process. Gauss view 05 was used to generate all the required models and the resulting structures were optimized in their electronic ground state. The optimized benzene ring cluster models are given in Fig. 1. The cluster models were named pristine activated biocarbon (AC), OH functionalized carbon (AC)OH, CHO functionalized carbon (AC)CHO and COOH functionalized carbon (AC)COOH.

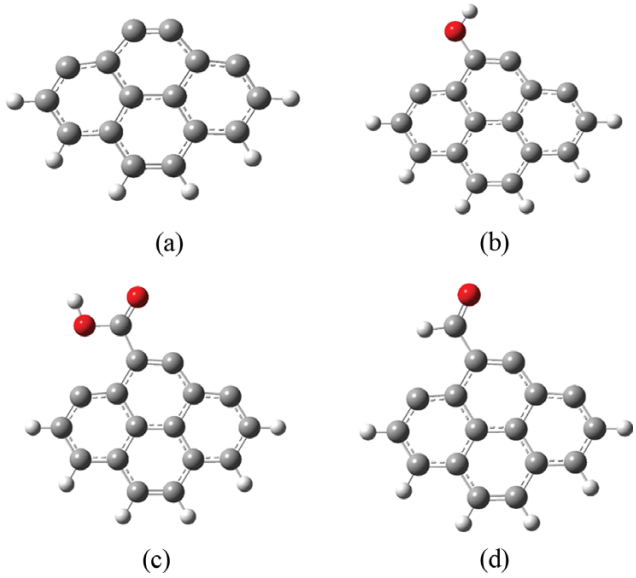

Fig. 1. The optimized model of (a) AC (b) (AC)OH (c) (AC)COOH (d) (AC)CHO.

The adsorption of 4-Nitrophenol at different sites of the carbon models was studied, and various possible ways of interaction were considered. The adsorption energy of 4-Nitrophenol on activated biocarbon surface was calculated by using the equation

$$E_{Ad} = E_{AB} - (E_A + E_B) \quad (9)$$

where, E_{AB} is the total energy of the 4-Nitrophenol and activated biocarbon system at equilibrium state; E_A is the total energy of the adsorbate 4-Nitrophenol, and E_B is the total energy of the activated biocarbon. Normally, the adsorption energy of less than −30 kJ/mol indicates a physisorptive interaction, whereas adsorption energy more than 50 kJ/mol indicates a chemisorptive type of interaction [37]. Besides, a higher negative value of adsorption energy would indicate stronger adsorption [41].

RESULTS AND DISCUSSION

1. Characterisation of RABC

The BET surface area and pore volume of RABC were found to be 919 m^2g^{-1} and 0.324 cm^3g^{-1}, respectively. The high surface area and pore volume of RABC indicate its good adsorptive nature. The surface morphology of the synthesized activated biocarbon observed under scanning electron microscopy revealed a non-uniform surface structure with cracks, cavities and pores. Fig. 2(a) gives the FESEM micrograph of the prepared activated biocarbon. The irregularities in the surface features could have arisen due to the combined effect of heat treatment and chemical activation. These processes result in the progressive elimination of volatile and disorganized matter, which ultimately creates cavities and voids. FTIR spectrum in Fig. 2(b) shows the presence of the different surface functional groups. The strong and broad band at around 3,443 cm^{-1} represents OH stretching vibration [45]. The two bands at 2,923 and 2,853 cm^{-1} may be due to C-H stretching vibration. The appearance of a peak at 1,741 cm^{-1} is assigned to C=O stretching vibration of aldehydes, ketones, esters and acetyl derivatives [46]. The peak at 1,625 cm^{-1} could be due to olefinic C=C stretching vibration, while the peak at around 1,463 cm^{-1} represents the skeletal C=C vibrations in aromatic rings [47]. The transmittance at 1,040 cm^{-1} is accounted to C-O stretching in alcohols, carboxylic acid or derivatives, phenols, ethers or esters group [48]. The bands between 800-500 cm^{-1} correspond to the vibrations of C-H, O-H and C-O bonds. The amorphous nature or crystalline nature of the prepared RABC was studied using XRD and Fig. 2(c) represents the X-ray diffractogram of the synthesized carbon. Two broad bands appearing at 2θ=~23° and ~43° could be attributed to the reflection from the (002) plane and (100) plane, respectively. The existence of such bands suggests the graphite-like microcrystallite structure of RABC [49]. The thermogravimetric analysis helps in comprehending the thermal stability and decomposition pattern of the activated biocarbon. Fig. 2(d) gives the thermogravimetric graph of RABC. A weight loss at temperatures below 200 °C could be due to loss of moisture present on the carbon [50]. The release of volatiles such as CO_2 and CO accounts for the weight loss at around 560 °C to 650 °C [51]. The retention of about 60% unburned weight at around 900 °C indicates the resistance of the RABC to a high heating condition, reflecting its excellent thermal-stable nature. The zero-point charge (pH_{ZPC}) of the RABC corresponds to 8.1. This means that at pH<8.1, the surface of the activated biocarbon will be positively charged, while at pH>8.1, the surface will possess nega-

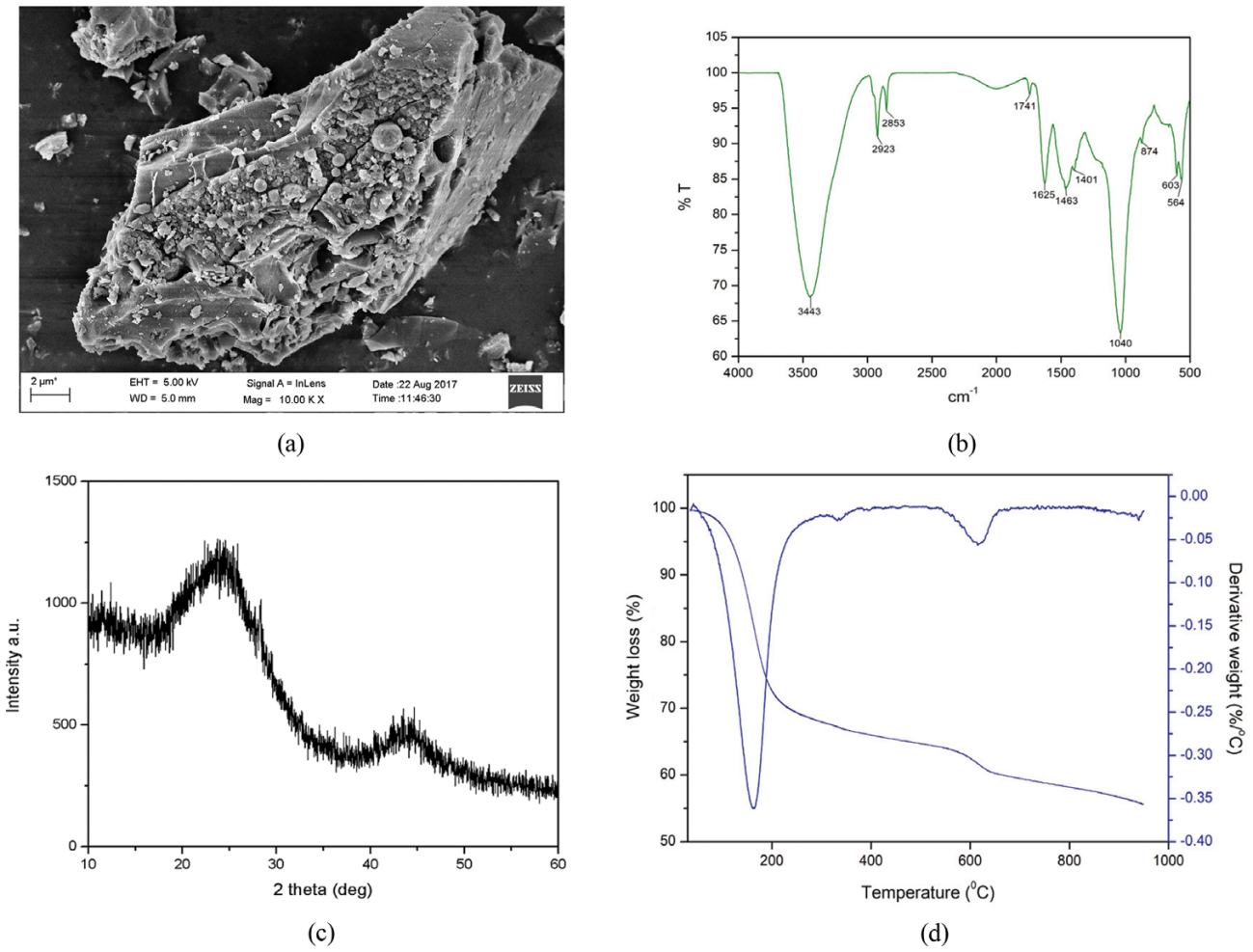

Fig. 2. (a) FESEM micrograph (b) FT-IR spectrum (c) XRD pattern (d) TGA/DTG profile of RABC.

tive charges.

2. Batch Adsorption Studies

The effect of adsorbent dose, contact time, initial concentration of 4-Nitrophenol and pH on the removal efficiency of 4-Nitrophenol from aqueous solution was investigated by batch adsorption method.

2-1. Effect of Adsorbent Dose

The adsorbent dose is one of the important factors in adsorption studies as it determines the capacity of activated biocarbon for the adsorption of an adsorbate. The optimum adsorbent dose was

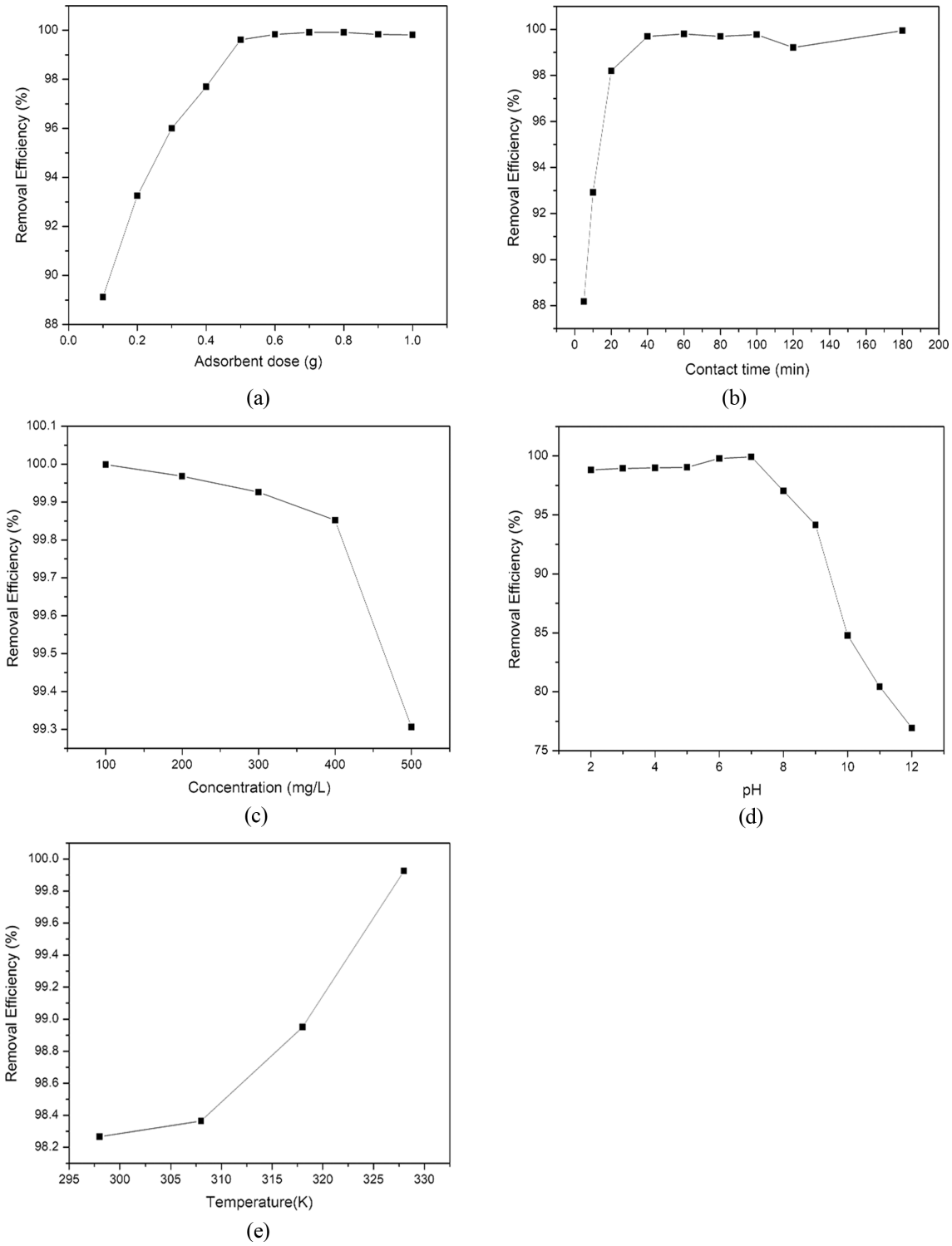

Fig. 3. (a) Effect of adsorbent dose (b) Effect of contact time (c) Effect of initial 4-Nitrophenol concentration and (d) Effect of pH and (e) Effect of temperature on 4-Nitrophenol adsorption.

obtained by varying the dosage of RABC from 0.1 to 1 g at pH-7, 25 °C temperature, initial 4-Nitrophenol concentration of 400 mg L^{-1} and 40 minutes contact time. As can be seen from Fig. 3(a), the removal percentage of 4-Nitrophenol increased from 89.11% to 99.6% with the increase in adsorbent dose from 0.1 g to 0.5 g. This increase in removal percentage may be due to the availability of more adsorption active sites and greater surface area at increased adsorbent dose [52]. However, the removal percentage remained almost constant above 0.5 g adsorbent dose, and this may be attributed to the aggregation or overlapping of available adsorption sites at higher adsorbent dose [53]. The adsorbent quantity of 0.5 g was chosen as the optimum dose for further studies.

2-2. Effect of Contact Time

The contact time helps determine the duration of equilibrium attainment between the adsorbate and adsorbent. The effect of contact time on removal efficiency was evaluated by variation of contact time (5 to 180 minutes) at constant adsorbent dosage (0.5 g), 400 mg L^{-1} initial 4-Nitrophenol concentration, pH-7 and 25 °C temperature. A plot of removal efficiency (%) of the RABC versus contact time is shown in Fig. 3(b). The uptake of 4-Nitrophenol increased rapidly at the initial period and gradually proceeded at a slower rate as the equilibrium was attained. The higher adsorption rate during the initial stages is associated with the availability of a large number of readily accessible sites on the adsorbent surface [54,55]. However, with the passage of contact time, the removal rate became slow, and finally, the system reached equilibrium after around 40 minutes. As time proceeds, the remaining vacant surface sites become less accessible as a result of the repulsive interaction between the 4-Nitrophenol molecules present on the adsorbent surface and in the solution, thereby decreasing the adsorption rate [56,57]. From the results, a contact time of 40 minutes was fixed as the optimum time for subsequent adsorption studies.

2-3. Effect of Initial Concentration

The effect of initial concentration on the adsorption of 4-Nitrophenol onto RABC was investigated at different 4-Nitrophenol concentrations ranging from 100 mg/L to 500 mg/L, while other parameters, i.e., adsorbent dose, contact time, temperature and pH, were fixed at 0.5 g, 40 minutes, 25 °C and 7, respectively. A plot of removal efficiency (%) versus the initial 4-Nitrophenol concentration is given in Fig. 3(c). It is clearly evident that the removal efficiency was inversely related to the initial concentration of 4-Nitrophenol. The higher removal percentage at lower 4-Nitrophenol concentrations may be due to the availability of more adsorption sites on the surface of the adsorbent than the number of adsorbate molecules present in the solution. However, at higher concentrations, the number of 4-Nitrophenol molecules competing for the same number of adsorption sites was higher, thus decreasing the removal efficiency [58].

2-4. Effect of pH

The pH of the solution plays a pivotal role in the process of adsorption. The effect of pH on the adsorption efficiency of 4-nitrophenol was determined by keeping all the other parameters at optimum conditions (adsorbent dose-0.5 g, 25 °C temperature, contact time - 40 minutes, initial concentration 400 mg/L) and varying the pH from 2 to 12. There was a slight increase in removal percentage of 4-Nitrophenol (98.8% to 99.9%) on increasing the pH from 2 to 7, whereas the removal efficiency decreased sharply when the pH of the solution increased to values higher than 7 (Fig. 3(d)). pKa value of 4-Nitrophenol was 7.15 while the pHzpc value of the RABC was found to be 8.1. Therefore, when the pH of the working solution was at pH less than 7, 4-Nitrophenol molecule would remain in its molecular form (pKa of 4-Nitrophenol=7.15) and the RABC surface had a positive charge ($pH<pH_{ZPC}$); as a result, there is an increase in the adsorptive interaction between 4-Nitrophenol and RABC. However, at pH more than 7, the surface of RABC would be negatively charge ($pH>pH_{ZPC}$), and the 4-Nitrophenol molecules will dissociate into ionic form since pH of the working solution is greater than the pKa value of 4-Nitrophenol. As a result, there will be a repulsive interaction between the 4-Nitrophenolate anions and the negatively charged carbon surface, which would eventually decrease the removal efficiency.

2-5. Effect of Temperature

The effect of temperature on the adsorption of 4-Nitrophenol was studied at four different temperatures: 298, 308, 318 and 328 K. The initial concentration of 4-Nitrophenol was set at 400 mg L^{-1}, contact time-40 minutes, pH-7 and 0.5 g adsorbent dose. Fig. 3(e) represents the plot of removal efficiency versus temperature. It is observed that the removal percentage of 4-Nitrophenol increased with the increase in temperature attaining a maximum of 99.9% was at 328 K.

3. Adsorption Isotherm Studies

Adsorption isotherm studies were conducted by fitting the adsorption equilibrium data into three commonly used isotherms: Langmuir, Freundlich and Temkin isotherm models. Table 1 presents the isotherm parameters and the chi-squared value for 4-Nitrophenol adsorption. From the R^2 value and chi-squared test (χ^2), it is observed that the Langmuir model best suited the experimental adsorption isotherm data, which signifies that 4-Nitrophenol adsorption onto the activated biocarbon proceeded through monolayer type of coverage. The value of maximum adsorption capacity (q_m) was 50.89 mg/g. The dimensionless separation value, R_L=0.001, signifies that the adsorption of 4-Nitrophenol is favourable. From the Freundlich analysis, it can be seen that the recipro-

Table 1. Adsorption isotherm parameters for 4-Nitrophenol adsorption onto RABC

Isotherm	Parameters	
Langmuir	q_m	50.890
	K_L	9.013
	R_L	0.001
	R^2	0.996
	χ^2	3.04×10^{-6}
Freundlich	1/n	0.208
	n	4.807
	K_F	39.417
	R^2	0.983
	χ^2	1.23×10^{-3}
Temkin	b_T	0.496
	A_T	29.591
	R^2	0.902
	χ^2	24.094

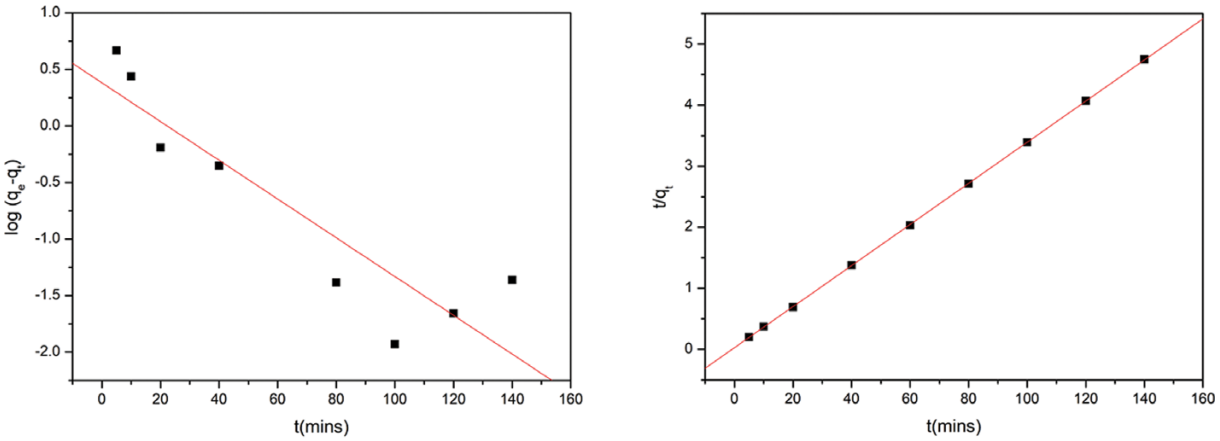

Fig. 4. Linear plot of (a) Pseudo-first-order and (b) Pseudo-second-order model for the adsorption of 4-Nitrophenol.

Table 2. Plot parameters of pseudo-first-order and second-order-model

Pseudo-first order					Pseudo-second order				
$q_{e,(exp)}$	$q_{e,(cal)}$	k_1	R^2	χ^2	$q_{e,(exp)}$	$q_{e,(cal)}$	k_2	R^2	χ^2
49.897	1.787	0.037	0.804	1.63×10^{-1}	49.897	49.900	0.113	0.999	1.06×10^{-5}

cal of Freundlich adsorption intensity value, 1/n, was found to be less than 1, which indicates that the adsorption follows normal Langmuir isotherm.

Chi-squared test was conducted to validate the isotherm models. The lowest χ^2 value was observed for Langmuir adsorption model, which suggests that the Langmuir isotherm best elucidated the adsorption of 4-nitrophenol onto the present activated biocarbon.

4. Adsorption Kinetic Studies

The kinetics of the adsorption process was studied by considering two kinetic models, pseudo-first-order and pseudo-second-order. The obtained kinetic graphs and their plot parameters are shown in Fig. 4 and Table 2, respectively. The experimental adsorption capacity value, $q_{e,(exp)}$, of pseudo-first-order model showed a vast difference from the calculated adsorption capacity value $q_{e,(cal)}$, which indicates the poor applicability of the pseudo-first-order model. However, for pseudo-second-order model, the $q_{e(exp)}$ was found to be in close agreement with the $q_{e,(cal)}$. Moreover, the highest R^2 value (0.999) and lowest chi-squared value ($\chi^2=1.06\times10^{-5}$) were obtained for the pseudo-second-order model. All these results indicate that pseudo-second-order kinetic model best elucidated the rate and mechanism of the 4-Nitrophenol adsorption, and thus, it can be concluded that chemisorption plays a vital role in the adsorption of 4-Nitrophenol.

5. Thermodynamic Study

The thermodynamics of the adsorption of 4-Nitrophenol onto RABC was studied from 298 K to 318 K. The thermodynamic parameters, such as enthalpy change (ΔH) and entropy change (ΔS), were calculated from the slope and intercept of the plot of $\ln K_d$ versus 1/T of Eq. (10), whereas the Gibbs free energy change (ΔG) at different temperatures was determined using Eq. (12). The obtained thermodynamic parameter values are given in Table 3.

Table 3. Thermodynamic parameters for 4-Nitrophenol adsorption onto RABC

ΔH (kJ mol^{-1})	ΔS (kJ mol^{-1} K^{-1})	ΔG (kJ mol^{-1})			
		298 K	308 K	318 K	328 K
50.80	0.17	0.06	−1.63	−3.34	−5.04

$$\ln K_d = \frac{\Delta S}{R} - \frac{\Delta H}{RT} \tag{10}$$

$$K_d = \frac{q_e}{C_e} \tag{11}$$

$$\Delta G = \Delta H - T\Delta S \tag{12}$$

where, K_d=distribution adsorption coefficient, q_e is the adsorbed 4-Nitrophenol concentration on RABC (mg g^{-1}), T is the absolute temperature (K), C_e is the concentration of 4-Nitrophenol at equilibrium (mg L^{-1}), ΔS corresponds to entropy change (kJ mol^{-1} K^{-1}), ΔG (kJ mol^{-1}) is Gibbs free energy change, ΔH represents the enthalpy change (kJ mol^{-1}), and R corresponds to the universal gas constant (8.314 kJ mol^{-1} K).

The value of change in enthalpy (ΔH) is positive, indicating that the adsorption of 4-Nitrophenol onto RABC is endothermic. The positive values of ΔS indicated increased randomness at the liquid and solid interface during the process of 4-Nitrophenol adsorption. The negative ΔG value implied the spontaneity of the adsorption process. Moreover, the ΔG value became more negative with increasing temperature, indicating that the adsorption of 4-Nitrophenol is more favorable at higher temperatures.

6. Theoretical Calculations

Density functional calculations were used to understand the

interactions taking place during the adsorption of 4-Nitrophenol onto RABC. Phenolic compounds may bind to the activated biocarbon surface in several ways, and most of the interactions proceed either through the aromatic ring of phenol or the hydroxyl group [36]. In this study, an attempt was made to understand the probable mechanism taking place during the adsorption of 4-Nitrophenol onto RABC via its hydroxyl group. Arm chair model was used to simulate pristine and functionalized activated biocarbon surface, and five different ways of interaction of 4-Nitrophenol with these activated biocarbon surfaces have been studied. Such studies broaden our understanding of the bonding and reactivity involved in adsorption process. Besides, the interaction studies of 4-Nitrophenol with the different functional group of activated biocarbon surface helps in identifying the functional group that would have the most significant impact on 4-Nitrophenol adsorption, and this would provide an idea for surface modification of activated biocarbon during its preparation process. The optimized structures for the 4-Nitrophenol adsorption on different activated biocarbon surfaces are given in Fig. 5, while the adsorption energies and bond distance between the adsorbate and adsorbent are given in Table 4.

6-1. 4-Nitrophenol Adsorption on Pristine Activated Biocarbon (AC)

The interaction of the hydroxyl group of 4-Nitrophenol (NP)OH with the pristine activated biocarbon was studied by considering the bond formation between the oxygen atom belonging to the

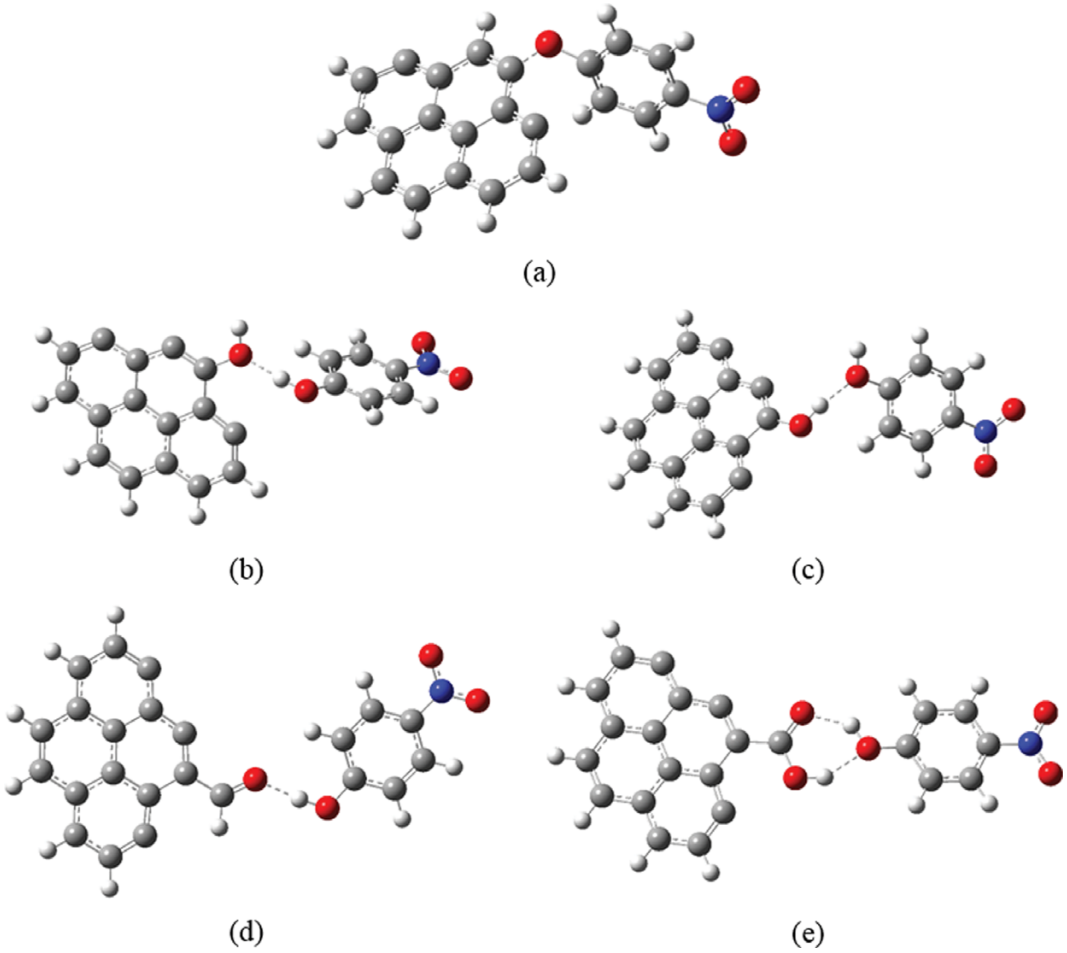

Fig. 5. Optimized structures of 4-Nitrophenol adsorption onto activated biocarbon (a) (AC)C---OH(NP) (b) (AC)HO---HO(NP) (c) (AC)OH---OH(NP) (d) (AC)CHO---HO(NP) (e) (AC)COOH---OH(NP).

Table 4. Adsorption energies and bond distance between 4-Nitrophenol and activated biocarbon systems

System	Mode of interaction	Adsorption energy (kJ/mol)	Bond length (Å)
NP+AC	(NP)HO----C(AC)	−313.54	1.40 (O_{NP}-C_{AC})
NP+(AC)OH	(NP)HO----HO(AC)	−31.56	1.72 (O_{NP}-H_{AC})
	(NP)OH----OH(AC)	−37.97	1.70 (H_{NP}-O_{AC})
NP+(AC)CHO	(NP)OH----OHC (AC)	−43.08	1.65 (H_{NP}-O_{AC})
NP+(AC)COOH	(NP)OH----HOOC(AC)	−45.18	1.74 (H_{NP}-O_{AC})
			1.77 (O_{NP}-H_{AC})

hydroxyl group of 4-Nitrophenol and the carbon atom of activated biocarbon surface (AC)C. The bond formation is represented as (NP)HO----C(AC) and the optimized structure is given in Fig. 5(a). It is clear from Fig. 5(a) that the OH group of 4-Nitrophenol molecule adsorbed dissociatively onto the arm chair model of activated biocarbon surface. The (NP)OH dissociates into (NP)O and H atom, resulting in the formation of two types of interactions: (NP)O----C(AC) and H_{NP}---C(AC). Moreover, the adjoining C-C bond length of the activated biocarbon surface where (NP)O and H atom were attached increased upon adsorption. This indicates that the electron cloud shifts towards the adsorption sites-(NP)HO----C(AC) resulting in weakening of the adjoining C-C bonds of the activated biocarbon surface. The adsorption energy corresponds to −313.54 kJ mol^{-1}, indicating that the 4-Nitrophenol adsorption on the pristine activated biocarbon is favorable and chemisorptive.

6-2. 4-Nitrophenol Adsorption on (AC)OH

The 4-Nitrophenol (NP)OH adsorption on the OH-functionalized activated biocarbon was studied by considering two types of interactions: (NP)HO----HO(AC) and (NP)OH----OH(AC). The optimized interaction structures of (NP)HO----HO(AC) and (NP)OH----OH(AC) are given in Fig. 5(b) and 5(c), respectively, and their corresponding bond lengths are given in Table 4. The adsorption energies of (NP)HO----HO(AC) and (NP)OH----OH(AC) interactions corresponded to −31.56 kJ/mol and −37.97 kJ/mol, respectively. The O_{NP}-H_{AC} bond length of (NP)HO----HO(AC) mode of interaction corresponded to 1.72 Å while H_{NP}-O_{AC} bond length of (NP)OH----OH(AC) corresponded to 1.70 Å. The higher negative value of adsorption energy and shorter bond length of (NP)OH----OH(AC) system indicates that (NP)OH----OH(AC) mode of interaction is more favorable than (NP)HO----HO(AC) type. Moreover, it can be deduced from the adsorption energy values of −31.56 kJ/mol and −37.97 kJ/mol that the interaction of hydroxyl group of 4-Nitrophenol with the OH-functionalized carbon is physisorptive.

6-3. 4-Nitrophenol Adsorption on (AC)CHO

The interaction of CHO-functionalized activated biocarbon with the hydroxyl group of 4-Nitrophenol (NP)OH resulted in the formation of (NP)OH----OHC(AC) complex. The interaction occurred between the hydroxyl hydrogen atom of 4-Nitrophenol and the oxygen atom of CHO-functionalized carbon surface (Fig. 5(d)). Such type of interaction increases the O-H bond length of 4-Nitrophenol from 0.97 Å to 1.02 Å and C=O bond length of CHO-functionalized carbon from 1.24 Å to 1.26 Å. Thus, the O-H bond of 4-Nitrophenol and C=O bond of functionalized carbon becomes weaker upon adsorption, and this may be due to the shifting of electron cloud more towards the adsorption site, i.e., O_{AC}-H_{NP} bond of (NP)OH----OHC(AC) system. The distance between the hydroxyl hydrogen atom of 4-Nitrophenol and oxygen atom of functionalized carbon was found to be 1.65 Å, while the adsorption energy corresponded to −43.08 kJ/mol. All these results indicate that the 4-Nitrophenol adsorption on CHO-functionalized carbon is favorable.

6-4. 4-Nitrophenol Adsorption on (AC)COOH

Adsorption of 4-Nitrophenol on COOH-functionalized activated biocarbon (AC)COOH proceeded through the formation of (NP)OH----HOOC(AC) complex. The optimized interaction structures are given in Fig. 5(e). The interaction occurred by forming two types of hydrogen bond between 4-Nitrophenol and COOH-functionalized carbon: one of the hydrogen bonds exist between the Hydroxyl hydrogen atom of 4-nitrophenol (NP)OH and the oxygen atom of COOH group of functionalized carbon surface (H_{NP}-O_{AC}), while the other bond exists between the hydroxyl oxygen atom of 4-Nitrophenol and the hydrogen atom of COOH group of functionalized activated biocarbon surface (O_{NP}-H_{AC}). The bond distance of H_{NP}-O_{AC} and O_{NP}-H_{AC} was found to be 1.74 Å and 1.77 Å, respectively, while the adsorption energy corresponded to −45.18 kJ/mol. Upon adsorption, the O-H bond length of both 4-Nitrophenol and (AC)COOH increased from 1.00 Å to 1.37 Å and from 0.98 Å to 1.00 Å, respectively. This indicates that the O-H bond becomes weaker as a result of the formation of H_{NP}-O_{AC} and O_{NP}-H_{AC} bond between 4-Nitrophenol and (AC)COOH. The interaction of 4-Nitrophenol with (AC)COOH was found to have the highest adsorption energy as compared to (AC)CHO and (AC)OH system. Thus, the high negative energy and decrease in bond length upon adsorption indicates that the interaction of 4-Nitrophenol with COOH-functionalized activated biocarbon is favorable.

A comparative study of the effect of functional groups on the 4-Nitrophenol adsorption was performed by considering their relative adsorption energies. The relative energy diagram of the optimized configurations of 4-Nitrophenol adsorption onto functionalized activated biocarbon system is Fig. 6. Among the various functional group considered for this study, the interaction of 4-Nitrophenol with (AC)COOH was found to possess the highest adsorption energy as compared to (AC)CHO and (AC)OH system. Hence, it can be assumed that the introduction of the carboxylic functional group into the activated biocarbon system would enhance the interaction of 4-Nitrophenol with the carbon surface more as compared to carbonyl and hydroxyl functional groups. The relative stability and energy of various configurations follow the order: (NP)OH----HOOC(AC)>(NP)OH----OHC(AC)>(NP)OH----OH(AC)>(NP)HO----HO(AC).

7. Comparative Study of Ravenna Grass Activated Biocarbon with Other Adsorbents

A comparative study of RABC with other adsorbent materials available in the literature was done to understand the relative efficiency of the obtained biocarbon for 4-Nitrophenol removal and is

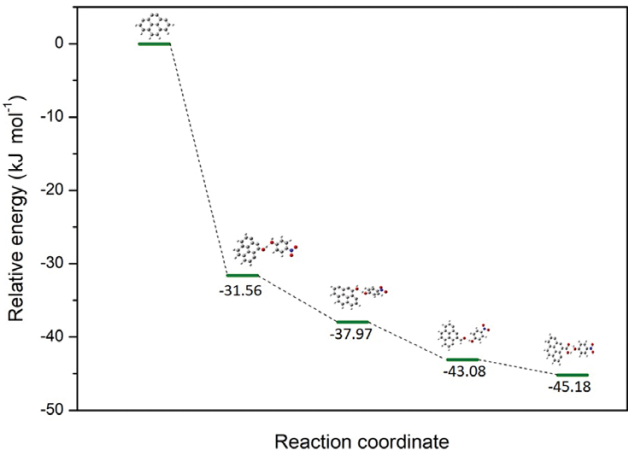

Fig. 6. Relative energy diagram of 4-Nitrophenol adsorption onto functionalized activated biocarbon.

Table 5. Comparison of RABC with some other adsorbent materials for 4-Nitrophenol removal

Adsorbent	Adsorbent characteristics		Adsorption capacity for 4-Nitrophenol removal q_{max} (mg g^{-1})	Source
	Surface area (m^2 g^{-1})	Pore volume (cm^3 g^{-1})		
RABC	919	0.324	50.89	Present study
Acacia glauca sawdust activated carbon	311.20	-	25.93	[33]
Mauritanian clay/alginate composite beads (Na-ZS26/SA)	-	-	27.1	[59]
Olive cake based activated carbon	672	-	1.550	[60]
Nano zirconium silicate coated manganese dioxide nanoparticles	-	-	2.619	[61]
Microporous activated carbon	780.06	0.468 (micro) 0.105 (meso)	184.86	[62]
Zeolite	-	-	1.02	[63]
Nanographite oxide	421.7	0.99	268.5	[64]
Eucalyptus seed derived carbon				
15% acid treated activated carbon	150	0.595	0.126	[65]
30% acid treated activated carbon	80	0.020	0.194	
15% base treated activated carbon	780	1.159	1.331	
30% base treated activated carbon	670	0.449	2.568	
Pyrolyzed oil shale	-	-	4.895	[66]
CO_2-oil shale	-	-	8.889	[66]
$ZnCl_2$-oil shale	-	-	0.026	[66]
KOH-oil shale	-	-	0.895	[66]
Metal-organic framework/reduced graphene oxide composite	0.66	-	327	[67]

shown in Table 5. The surface area and maximum adsorption capacity of adsorbent materials were considered for the comparison. From Table 5, it can be seen that the RABC has comparatively high surface area of 919 m^2 g^{-1} and adsorption capacity of 50.85 mg g^{-1}, respectively, as compared to other adsorbent. This shows that the activated biocarbon obtained from this study could be used as an efficient adsorbent for 4-Nitrophenol removal from water.

8. Cost analysis

The total approximate cost involved in the production of 250 gram of the RABC was calculated, which included the price of KOH, electricity, water, HCl and raw precursor. The resulting production cost was subsequently compared with that of commercially available carbon to draw a comparison with regard to economic feasibility. Table 6 presents the cost of the RABC, while Fig. S1 (supplementary Fig. 1) represents the relative cost of different carbon in terms of Rupees (₹). In the present study, around 1.4 kg of raw material was used for the production of 0.250 kg of activated biocarbon. The cost involved in the production of 250 g RABC was found to be (₹) 538 without considering the cost involved in initial investment, labor income, working capital, manufacturer's profits, recovery and reuse of KOH. This production cost is expected to be reduced in scaling up from laboratory experiments to industrial scale. A comparative study of the production cost indicates that Ravenna grass activated biocarbon could be one of the most economical among all other commercially available carbons considered for this study.

Table 6. Cost estimates for production of 250 g RABC

Materials	Consumption (approx.)	Cost (approx.)
KOH	500 g	₹ 480
HCl	200 ml of 0.1 M HCl	₹ 1 (₹ 265/500 ml)
Raw precursor	1.4 kg	₹ 0
Electricity	14 kWh	₹ 42
Water	50 L	₹ 15
Total Cost/250 g (in Rupees)	-	₹ 538

*1 dollar ($)=Approx.72.00 Rupees (₹)

CONCLUSION

Ravenna grass biomass served as a potent precursor for the preparation of activated biocarbon. Surface area, pore volume and zero-point charge of the prepared carbon were found to be 919 m^2g^{-1}, 0.324 cm^3g^{-1} and 8.1 respectively. XRD analysis revealed the microcrystallite structure of the RABC, while SEM image indicated the presence of numerous voids, cracks and cavities on the carbon surface. The Ravenna grass activated biocarbon could serve as a good adsorbent for removal of 4-Nitrophenol from aqueous solution. At best conditions (adsorbent dose-0.5 g, pH-7, contact time-40 minutes, initial 4-Nitrophenol concentration - 400 mgL^{-1}), the activated biocarbon exhibited a maximum removal percentage of 99.9%. The

adsorption capacity was greatly influenced by the pH_{zpc} of the activated biocarbon and the pH of the working solution. The removal percentage decreased sharply when the pH value was increased from 7 to 12. The Langmuir model best explained the equilibrium isotherm with q_m of 50.89 mgg^{-1}, while pseudo-second-order model well described the kinetics data. The thermodynamics study indicated the temperature dependence, spontaneity and endothermic nature of the adsorption process. Density functional theory calculations also revealed the favorable adsorption of 4-Nitrophenol onto pristine and functionalized activated biocarbon. Among the different functional groups used to functionalize the activated biocarbon (-OH, -CHO, -COOH), the -COOH group interacted most strongly with 4-Nitrophenol. These results indicate that functionalization of activated biocarbon with COOH group would increase its interaction with 4-Nitrophenol, which would eventually improve the adsorption properties.

ACKNOWLEDGEMENT

The authors Aola Supong and Parimal Chandra Bhomick are grateful to the Department of Science and Technology-INSPIRE Fellowship. The authors also acknowledge Department of Chemistry, Calcutta University for computational facilities. The support received under DST-FIST is also acknowledged.

CONFLICT OF INTEREST

The authors declare that they have no conflict of interest.

SUPPORTING INFORMATION

Additional information as noted in the text. This information is available via the Internet at http://www.springer.com/chemistry/journal/11814.

REFERENCES

1. N. G. Rincón-Silva, J. C. Moreno-Piraján and L. Giraldo, *Adsorption*, **22**, 33 (2016).
2. I. Ipek, N. Kabay and M. Yüksel, *J. Water Process Eng.*, **16**, 206 (2017).
3. R. R. Karri, J. N. Sahu and N. S. Jayakumar, *J. Taiwan Inst. Chem. Eng.*, **80**, 472 (2017).
4. E. Z-Flores, M. Abatal, A. Bassam, L. Trujillo, P. Juárez-Smith and Y. El Hamzaoui, *J. Clean. Prod.*, **161**, 860 (2017).
5. A. Sukan and S. Sargin, *J. Biomater. Nanobiotechnol.*, **4**, 300 (2013).
6. L. G. C. Villegas, N. Mashhadi, M. Chen, D. Mukherjee, K. E. Taylor and N. Biswas, *Curr. Pollut. Reports*, **2**, 157 (2016).
7. E. Yagmur, S. Turkoglu, A. Banford and Z. Aktas, *J. Clean. Prod.*, **149**, 1109 (2017).
8. S. K. Nadavala, H. Che Man and H. Woo, *BioResources*, **9**, 5155 (2014).
9. A. Q. Jaradat, S. Gharaibeh and M. Abu Irjei, *Water Environ. J.*, **32**, 134 (2018).
10. Y. Jiang, G. Ni, G. Zhao, Y. Meng, J. Li and X. Wang, *Plasma Process. Polym.*, **10**, 353 (2013).
11. F. Khazaali, A. Kargari and M. Rokhsaran, *Desalin. Water Treat.*, **52**, 7543 (2013).
12. Y. Wu, G. Tian, H. Tan and X. Fu, *Desalin. Water Treat.*, **51**, 37 (2013).
13. N. Rabaaoui, M. E. K. Saad, Y. Moussaoui, M. S. Allagui, A. Bedoui and E. Elaloui, *J. Hazard. Mater.*, **250-251**, 447 (2013).
14. M. Tian, S. S. Thind, J. S. Dondapati, X. Li and A. Chen, *Chemosphere*, **209**, 182 (2018).
15. V. Peings, J. Frayret and T. Pigot, *J. Environ. Manage.*, **157**, 287 (2015).
16. Y. Song, J. Jiang, J. Ma, S. Y. Pang, Y. Z. Liu, Y. Yang, C. W. Luo, J. Q. Zhang, J. Gu and W. Qin, *Environ. Sci. Technol.*, **49**, 11764 (2015).
17. Y. Tu, Y. Xiong, S. Tian, L. Kong and C. Descorme, *J. Hazard. Mater.*, **276**, 88 (2014).
18. M. Kuosa, J. Kallas and A. Häkkinen, *J. Environ. Chem. Eng.*, **3**, 325 (2015).
19. M. Madani, M. Aliabadi, B. Nasernejad, R. K. Abdulrahman, M. Y. Kilic and K. Kestioglu, *Desalin. Water Treat.*, **53**, 2031 (2015).
20. K. Akin, I. Arslan-Alaton, O. H. Tugba and M. Bekbolet, *Chem. Eng. J.*, **224**, 4 (2013).
21. G. Moussavi, S. Ghodrati and A. Mohseni-Bandpei, *J. Biotechnol.*, **184**, 111 (2014).
22. H. Jalayeri, F. Doulati Ardejani, R. Marandi and S. Rafiee pur, *Arab. J. Geosci.*, **6**, 3847 (2013).
23. D. Y. Xu and Z. Yang, *Chemosphere*, **92**, 391 (2013).
24. J. A. Torres, P. M. B. Chagas, M. C. Silva, C. D. Dos Santos and A. D. Corrêa, *Environ. Technol. (United Kingdom)*, **37**, 1288 (2016).
25. S. Aber, A. Khataee and M. Sheydaei, *Bioresour. Technol.*, **100**, 6586 (2009).
26. H. Fan, L. Shi, H. Shen and K. Xie, *RSC Adv.*, **6**, 109983 (2016).
27. B. Li, *Energy Environ. Sci.*, **9**, 102 (2016).
28. K. Ngaosuwan, J. G. Goodwin and P. Prasertdham, *Renew. Energy*, **86**, 262 (2016).
29. A. Mullick, S. Moulik and S. Bhattacharjee, *Indian Chem. Eng.*, **60**, 58 (2017).
30. N. You, J. Li, H. Fan and H. Shen, *J. Adv. Res.*, **15**, 77 (2018).
31. G. Selvaraju, N. Kartini and A. Bakar, *J. Clean. Prod.*, **141**, 989 (2016).
32. A. Kumar and H. M. Jena, *J. Clean. Prod.*, **137**, 1246 (2016).
33. P. T. Dhorabe, D. H. Lataye and R. S. Ingole, *Water Sci. Technol.*, **73**, 955 (2016).
34. X. Liu, F. Wang and S. Bai, *Water Sci. Technol.*, **72**, 2229 (2015).
35. P. T. Dhorabe, D. H. Lataye and R. S. Ingole, *J. Hazardous, Toxic, Radioact. Waste*, **21**, 4016015 (2017).
36. L. M. Cam, L. Van Khu and N. N. Ha, *J. Mol. Model.*, **19**, 4395 (2013).
37. F. Shen, J. Liu, Z. Zhang, Y. Dong and C. Gu, *Fuel Process. Technol.*, **171**, 258 (2018).
38. B. Padak, M. Brunetti, A. Lewis and J. Wilcox, *Environ. Prog.*, **25**, 319 (2006).
39. L. R. Radovic, *Carbon N. Y.*, **43**, 907 (2005).
40. D. Cortés-Arriagada, L. Sanhueza and M. Santander-Nelli, *J. Mol. Model.*, **19**, 3569 (2013).
41. J. Liu, W. Qu, S. W. Joo and C. Zheng, *Chem. Eng. J.*, **184**, 163 (2012).
42. B. M. Babic, S. K. Milonjic, M. J. Polovina and B. V. Kaludierovic, *Carbon N. Y.*, **37**, 477 (1999).

43. Y. S. Ho, G. McKay, D. A. J. Wase and C. F. Forster, *Adsorpt. Sci. Technol.*, **18**, 639 (2000).
44. M. J. Frisch, G. W. Trucks, H. B. Schlegel, G. E. Scuseria, M. A. Robb, J. R. Cheeseman, G. Scalmani, V. Barone, B. Mennucci, G. A. Petersson, H. Nakatsuji, M. Caricato, X. Li, H. P. Hratchian, A. F. Izmaylov, J. Bloino, G. Zheng, J. L. Sonnenberg, M. Hada, M. Ehara, K. Toyota, R. Fukuda, J. Hasegawa, M. Ishida, T. Nakajima, Y. Honda, O. Kitao, H. Nakai, T. Vreven, J. A. Montgomery Jr., J. E. Peralta, F. Ogliaro, M. Bearpark, J. J. Heyd, E. Brothers, K. N. Kudin, V. N. Staroverov, R. Kobayashi, J. Normand, K. Raghavachari, A. Rendell, J. C. Burant, S. S. Iyengar, J. Tomasi, M. Cossi, N. Rega, J. M. Millam, M. Klene, J. E. Knox, J. B. Cross, V. Bakken, C. Adamo, J. Jaramillo, R. Gomperts, R. E. Stratmann, O. Yazyev, A. J. Austin, R. Cammi, C. Pomelli, J. W. Ochterski, R. L. Martin, K. Morokuma, V. G. Zakrzewski, G. A. Voth, P. Salvador, J. J. Dannenberg, S. Dapprich, A. D. Daniels, Ö. Farkas, J. B. Foresman, J. V Ortiz, J. Cioslowski and D. J. Fox, *Gaussian Inc., Wallingford CT*, Wallingford CT (2009).
45. M. L. Martínez, M. M. Torres, C. A. Guzmán and D. M. Maestri, *Ind. Crops Prod.*, **23**, 23 (2006).
46. I. I. Gurten, M. Ozmak, E. Yagmur and Z. Aktas, *Biomass Bioenergy*, **37**, 73 (2012).
47. J. Matos, C. Nahas, L. Rojas and M. Rosales, *J. Hazard. Mater.*, **196**, 360 (2011).
48. D. Angin, *Fuel*, **115**, 804 (2014).
49. S. Li, K. Han, J. Li, M. Li and C. Lu, *Micropor. Mesopor. Mater.*, **243**, 291 (2017).
50. B. H. Diya'uddeen, I. A. Mohammed, A. Ahmed and B. Y. Jibril, *Agric. Eng. Int.*, **10**, 1 (2008).
51. J. Bartram and R. Ballance, *Water Quality Monitoring: A Practical Guide to the Design and Implementation of Freshwater Quality Studies and Monitoring Programmes*, 1st Ed. (E & FN Spon, 1996).
52. H. Soni and P. Padmaja, *J. Porous Mater.*, **21**, 275 (2014).
53. H. Moazed and S. B. Nasab, *J. Mol. Liq.*, **211**, 448 (2015).
54. D. Balarak, *Int. J. ChemTech Res.*, **9**, 681 (2016).
55. S. N. Muluh, J. N. Ghogomu, A. A. B. Alongamo and D. L. Ajifack, *Int. J. Adv. Eng. Res. Technol.*, **5**, 610 (2017).
56. M. Shirzad-Siboni, S.-J. Jafari, M. Farrokhi and J. K. Yang, *Environ. Eng. Res.*, **18**, 247 (2013).
57. D. Kavitha, *J. Environ. Biotechnol. Res.*, **3**, 24 (2016).
58. P. Sudhakar, I. D. Mall and V. C. Srivastava, *Desalin. Water Treat.*, **57**, 12375 (2016).
59. A. Ely, M. Baudu, M. Ould, S. Ahmed, O. Kankou and J. Basly, *Chem. Eng. J.*, **178**, 168 (2011).
60. E. S. A. Rawash, *Glob. J. Environ. Sci. Manag.*, **2**, 11 (2016).
61. M. E. Mahmoud and G. M. Nabil, *J. Mol. Liq.*, **240**, 280 (2017).
62. M. J. Ahmed and S. K. Theydan, *Desalin. Water Treat.*, **55**, 522 (2015).
63. T. Sismanoglu and S. Pura, *Colloids Surfaces A Physicochem. Eng. Asp.*, **180**, 1 (2001).
64. B. Zhang, F. Li, T. Wu, D. Sun and Y. Li, *Colloids Surfaces A Physicochem. Eng. Asp.*, **464**, 78 (2015).
65. N. G. Rincón-Silva, J. C. Moreno-Piraján and L. G. Giraldo, *J. Chem.*, **2015**, 1 (2014).
66. S. Al-Asheh, B. Fawzi and M. Asmahan, *Environ. Geol.*, **45**, 1109 (2004).
67. Z. Wu, X. Yuan, H. Zhong, H. Wang and G. Zeng, *Nat. Publ. Gr.*, **6**, 25638 (2016).

Supporting Information

A combined experimental and theoretical investigation of the adsorption of 4-Nitrophenol on activated biocarbon using DFT method

Aola Supong, Parimal Chandra Bhomick, Upasana Bora Sinha, and Dipak Sinha[†]

Department of Chemistry, Nagaland University, Lumami-798627, India
(*Received 16 May 2019 • accepted 2 September 2019*)

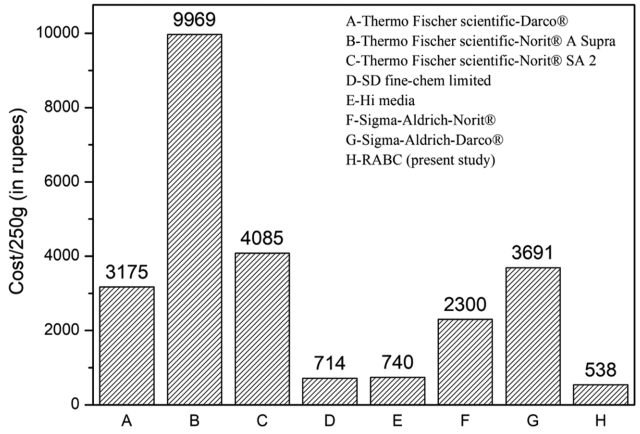

Fig. S1. Comparative cost of Ravenna grass activated biocarbon with some commercially available activated carbon.